Virus Genes (2009) 38:19–29
DOI 10.1007/s11262-008-0304-3

Genome-wide reduction in transcriptomal profiles of varicella-zoster virus vaccine strains compared with Parental Oka strain using long oligonucleotide microarrays

Esther Grinfeld · Alan Ross · Thorsten Forster · Peter Ghazal · Peter G. E. Kennedy

Received: 27 August 2008 / Accepted: 10 November 2008 / Published online: 27 November 2008

Abstract Varicella-Zoster virus (VZV) causes varicella as a primary infection following which it becomes latent in human ganglia and then reactivates to cause herpes zoster. VZV vaccines are used to prevent primary infection with varicella, and also to reduce the incidence of viral reactivation causing herpes zoster and post-herpetic neuralgia. To gain further insights into the molecular basis of their attenuated virulence, we used long oligonucleotide microarrays to determine the lytic transcriptomal profiles of two vaccine VZV strains (Merck and GSK) compared with the Oka parental (P-Oka) strain. There was a global downregulation of transcription of both vaccines relative to P-Oka, although this downregulation was more extensive in the GSK strain. Open Reading Frames (ORFs) 62 and 14 were the most transcriptionally downregulated on the arrays for both vaccines compared with the parental strain.

Keywords Varicella-zoster virus · Microarray · Genome · Open reading frame

Introduction

Varicella-Zoster virus (VZV) is a human herpes virus that causes varicella (chickenpox) as a primary infection, and following a variable period of latency in ganglionic neurons, it reactivates to cause herpes zoster (shingles) [1–3]. Both varicella and herpes zoster may be associated with significant neurological complications especially in the immunosuppressed [4], and VZV reactivation may be followed by post-herpetic neuralgia that can be very refractory to treatment, myelitis, and both small and large vessel vasculopathy [5]. There is considerable interest in the use of live attenuated VZV vaccines both to prevent varicella in the context of an established childhood vaccination policy, and in the prevention of herpes zoster and resultant post-herpetic neuralgia in individuals over 60 years [6, 7]. While VZV vaccine has been shown to contain at least 42 loci that differ from the parental (P-Oka) strain [8], the precise basis of the attenuation of the vaccine virus is not understood. We therefore undertook a study using recently constructed long oligonucleotide VZV microarrays of the transcriptomal profiles of two VZV vaccines in current use and compared them with those of the P-Oka strain during lytic infection of MeWo cells. We hypothesised that both vaccines would show significant differences in their transcriptional activity compared with the parental virus.

E. Grinfeld · P. G. E. Kennedy (✉)
Department of Neurology, Division of Clinical Neurosciences, Institute of Neurological Sciences, Southern General Hospital, Glasgow G51 4TF, Scotland, UK
e-mail: P.G.Kennedy@clinmed.gla.ac.uk

A. Ross · T. Forster · P. Ghazal
Division of Pathway Medicine, University of Edinburgh Medical School, The Chancellor's Building, Little France Crescent, Edinburgh EH16 4SB, Scotland, UK

Materials and methods

Viruses and cells

MeWo cells (a human melanoma cell line) were grown in Gibco 1966 DMEM medium containing glutamine, non-essential amino acids, 10% foetal calf serum (FCS), and gentamicin. A total of 3×10^6 MeWo cells were mixed with an equal number of MeWo cells infected with similar amounts (confirmed by DNA PCR) of either P-Oka, a gift

from Dr. J. I. Cohen, Merck vaccine (Varivax) or GSK vaccine (Varilrix) strains which had previously been grown on MeWo cells, grown in T175 flasks. Since all three viruses were treated in the same way, it was not thought that the composition of the initial inoculum 50:50 ratio had an additional effect on the differences observed after 72 h. By 72 h a >90% viral infection was achieved, meaning that (approximately) 90% of the cells were infected with VZV, and the cells trypsinised and RNA extracted from 10^7 cells pelleted and resuspended in lysis buffer containing β-mercaptoethanol. The samples were placed on a QIAshredder spin column and centrifuged at maximum speed for 2 min. An equal volume of 70% ethanol was added to the flow-through which was placed on the Qiagen column from a DNeasy kit (Qiagen), washed as per the manufacturers instructions, and then DNase (Qiagen RNase-free DNase) was added to the column. After several washes, the RNA was eluted and was DNase-treated again (DNA-free kit, Ambion) at 37° as per the manufacturers instructions. The absence of residual DNA was shown by PCR for β-actin. c-DNA was synthesised using Superscript II (Invitrogen) on RNA primed with poly-dT and random primers. RT-PCR was performed on all samples, and as a further check for DNA contamination, PCR was also performed on samples which were not reverse transcribed. To obtain the results reported below, a total of five 250 ml flasks of VZV-infected and five flasks of non-infected MeWo cells were harvested at 72 h. Each virus was passaged five times in MeWo cells. The pooled data from these experiments were then statistically analysed as described below to obtain the final results.

Probe design and array fabrication

The methodology of probe design and array fabrication for these experiments has been previously described [9]. The sequences of all the oligonucleotides used in these VZV arrays together with the detailed rationale underlying their design and construction has been previously detailed in this previous account [9]. In brief, probes were designed using Oligo 6 software (Molecular Biology Insights, Inc.), and Open Reading Frame (ORF)- and strand-specific viral probe sequences were based on the original sequencing data of the Dumas strain [10]. The 24 negative controls for this study were Murine Cytomegalovirus (CMV), and there were 13 positive controls (shown in Table 1). Probes were synthesised by MWG-biotech, resuspended at 100 μM in printing buffer containing 50% glycerol and 0.01% triton X-100 and robotically printed using an Arrayjet Aj120 Super marathon (Arrayjet Limited) using inkjet non-contact technology with 15 array repeats per slide onto γ-aminopropylsilane (GAPS) II-coated slides (Corning Inc.). Quality control of the arrays was carried out using spotcheck (random 9 mers hybridisation) and stored under nitrogen at room temperature prior to use.

Array hybridisation

The Cy3 target cRNAs were hybridised to the arrays, washed, and scanned using an Agilent microarray scanner. Array hybridisation and analysis followed standard operating procedures [11]. Each type of sample had multiple ($n = 5$) biological replicate arrays. 750 ng of total RNA, from each sample, was labelled using an Agilent low input linear amplification kit (Agilent Technologies UK Ltd. 5184-3523). A primer containing poly-dT and a T7 polymerase is annealed to the ploy A RNA. Reverse transcriptase is added to synthesise the first and second strand cDNA. cRNA is synthesised from the double stranded cDNA using T7 polymerase which simultaneously incorporates a cyanine dye labelled CTP. 3 μg of the Cyanine3 labelled cRNA was hybridised to each array for 16 h at 60 degrees in a rotating oven.

The arrays were washed to remove unbound cRNA and dried before scanning using an Agilent slide scanner G2565A.

The scanner uses dynamic autoFocus (continually adjusts scanner's focus, keeping features in focus at all times) and the scan was at 5 micron resolution, using a SHG-YAG laser, 532 nm to detect the Cyanine 3 (550 excitation 570 emission).

Image (image quantification) analysis was done using Quantarray (version 3.0.0) imaging software from Packard Bioscience.

Data processing and normalisation

We used a robust statistical model that pools variance estimates from multiple ORFs, which also alleviates data variation issues with small sampler sizes. To define the linear dynamic range of Cy3 and to control for scanning parameters, arrays were scanned with increasing settings to generate five datasets which were then analysed against each other by scatter plots. Optimal scans with large dynamic range but without signal saturation were selected. Data processing and analysis were undertaken with R Language and Environment for Statistical Computing, and comprised the stages described here. The contribution of background noise to measured signal intensity was addressed by subtracting individual background readings from each probes' intensity measurements. Where these corrected values are 0 or negative, they were replaced by a constant value of 1, before a $\log_2$ transformation of all data points. A between-array normalisation based on whole-array data distributions was counter-indicated for this viral array, given that more than 5–10% of the ORFs could be

Table 1 Positive and negative control probes used in study

Positive control probes	
1	GAPDH
2	Myosin light chain, alkali, Alt. splice 2
3	MHC-1
4	Ribosomal protein S16
5	Beta-actin
6	P52 and p64 isoforms of N-Shc
7	Alphatubulin
8	3 Cab mRNA for photosystem I chlorophyll
9	Lysosolmal hyaluronidase
10	EF1-alpha
11	3 Athb-2 mRNA
12	Homologue to yeast ribosomal protein L41
13	3 HAT4
Negative control probes	
1	Arabidopsis thaliana (rbcL)
2	Arabidopsis thaliana mRNA for rubisco activase
3	Arabidopsis thaliana fructose-bisphosphatase-like
4	NEG1_CCATTAACTTGCACAAAAGAGTATGTGAAAGAATAAAAATATAATGCC
5	Arabidopsis thaliana clone HAT1 homeobox protein m
6	NEG25_TGTAATATGAGAATCAAACTTAAATATATCCTATACTAACAATTT
7	Arabidopsis thaliana putative beta-amylase (At5g55)
8	NEG13_TTGAAAATTCGAGGAAAATATCTGTGGCTAGCAGTAGGGG
9	NEG37_TTACAAGTTTTGCCTTTAGAAGATCACATCGTACTAACGAGCCCTTG
10	NEG74_TGAGCCATCATGAAGTTGAACATTTCTTACCCAGTCAACG
11	NEG3_CAATTGGTTGACTTGAAAAAGGAGTTGGCTGAATTGAAGG
12	NEG50_CCATTGATTGTTGTTGAATGTTTCTGACGACGTGCAAGAT
13	NEG27_AATAATCTTTATAATTTTATAATGGAAAGTAATTTGACTAAAG
14	NEG86_GGTGCCGTCCATCTTTCTACTTACTTGAAGGTCTACAA
15	NEG15_TTGAAAGAAACTATAGCTAAATAATATATACAAAATGGCTCACGAAAA
16	NEG62_GATTTTATGCCAAACCAGTTAAGAAAGCTGATGGGTCCAT
17	NEG39_CTGCCTCCAAACAAAGCTATTCTCGTCCTAGCGCTCCACC
18	NEG73_CCTTGTAATTTACGTTTCCTTAAATCTTCTTTCTACTAACGTTTT
19	NEG2_TGTGGGGGTTATATATTGTCGTCTTTCTTTTAACATTCAATAATG
20	NEG49_AATCGTTATTTGAAATATAGTATCGCTTCGCAACCAAGAA
21	NEG26_CTGCCGTCCCAAGTGTCCAAACTTTTGGTAAGAAGAAATC
22	NEG85_CGACTTTTTCGCAAAAACATTAACATATATAAAACTAGCG
23	NEG14_TGGCGGAGATAGATAAATTATCGAAAAAGGTTCTTAGTTT
24	NEG61_CAATCAGTTCCTGGAGATGTACGTAACGACCCCTCAAA

expected to have changed transcription levels between different biological conditions. Instead, scaling of individual arrays to a constant set of positive controls was used. Of the 13 individual positive controls identified on the array, a set of seven positive controls (each with 15 replicate prints per array) was chosen to represent a stable between-array normalisation reference. The normalisation constant for each array was calculated (in $\log_2$ scale) as the difference between a reference value and the 75th percentile of the set of selected 90 positive control spots on an array. The reference value is the average of all arrays 75th percentile values calculated on the same control spots. Given that each probe on the array has 15 print replicates, we robustly estimated expression for a unique transcript as the median intensity of its replicate prints.

Analysis

Expression and non-expression for individual samples was calculated by comparing each transcripts expression level against the detection threshold delta for that array. Delta is in turn calculated as median + 2 median absolute

Table 2 Differential transcription between parental Oka and Merck vaccine samples

	Log_2 fold change pOKA versus Merck vaccine	Log_2 expression in pOKA	Log_2 expression Merck	Antilogged fold change	*P*-value	FDR *P*-value
ORF18	0.59	8.8	9.4	1.51	0.080	0.210
ORF27	0.53	11.5	12.0	1.44	*	0.123
ORF24	0.24	12.5	12.7	1.18	0.379	0.576
ORF57	0.22	12.4	12.6	1.16	0.359	0.556
ORF49	0.14	14.2	14.3	1.10	0.516	0.694
ORF63	0.10	12.2	12.3	1.07	0.661	0.817
ORF19	0.09	6.8	6.9	1.06	0.637	0.816
ORF26	0.08	6.7	6.8	1.05	0.767	0.886
ORF15	0.08	10.4	10.4	1.05	0.673	0.817
ORF30	0.07	6.9	6.9	1.05	0.726	0.863
ORF31	0.07	7.8	7.9	1.05	0.630	0.816
ORF11c	0.07	10.8	10.9	1.05	0.677	0.817
ORF70	0.06	8.5	8.5	1.04	0.781	0.890
ORF51	0.05	5.8	5.9	1.04	0.751	0.880
ORF44	0.05	8.3	8.3	1.03	0.824	0.903
ORF7	0.03	12.0	12.1	1.02	0.832	0.903
ORF9	0.03	12.7	12.7	1.02	0.861	0.903
ORF16	0.02	8.3	8.4	1.01	0.897	0.920
ORF64	0.01	12.4	12.4	1.01	0.968	0.968
ORF50a	−0.01	11.6	11.5	0.99	0.950	0.961
ORF67	−0.03	6.2	6.2	0.98	0.870	0.903
ORF11a	−0.04	6.3	6.3	0.97	0.857	0.903
ORF45	−0.06	8.2	8.2	0.96	0.797	0.895
ORF37	−0.07	7.0	6.9	0.95	0.862	0.903
ORF39	−0.07	7.2	7.1	0.95	0.677	0.817
ORF66	−0.09	4.8	4.7	0.94	0.606	0.802
ORF10	−0.15	10.8	10.7	0.90	0.354	0.556
ORF8	−0.15	9.4	9.3	0.90	0.496	0.677
ORF47	−0.16	6.8	6.6	0.90	0.405	0.585
ORF28	−0.16	9.3	9.1	0.89	0.360	0.556
ORF17	−0.17	8.7	8.5	0.89	0.330	0.541
ORF46b	−0.17	5.7	5.5	0.89	0.407	0.585
ORF11b	−0.17	8.3	8.2	0.89	0.436	0.612
ORF1a	−0.19	6.9	6.7	0.88	0.398	0.585
ORF48b	−0.19	13.0	12.8	0.88	0.304	0.515
ORF40	−0.22	8.0	7.8	0.86	0.176	0.328
ORF13b	−0.23	10.9	10.6	0.85	0.267	0.465
ORF5	−0.24	7.3	7.1	0.85	0.440	0.612
ORF69	−0.24	12.2	11.9	0.84	0.258	0.460
ORF32	−0.28	11.4	11.1	0.82	0.108	0.241
ORF38	−0.29	11.6	11.3	0.82	0.065	0.185
ORF36	−0.29	4.3	4.0	0.82	0.160	0.319
ORF20	−0.30	10.1	9.8	0.81	0.085	0.210
ORF43	−0.32	6.5	6.2	0.80	0.308	0.515
ORF12	−0.32	6.6	6.3	0.80	0.068	0.185
ORF53	−0.33	11.5	11.2	0.80	0.193	0.352
ORF4b	−0.33	9.4	9.0	0.79	0.173	0.328

Table 2 continued

	Log_2 fold change pOKA versus Merck vaccine	Log_2 expression in pOKA	Log_2 expression Merck	Antilogged fold change	*P*-value	FDR *P*-value
ORF46a	−0.33	7.6	7.3	0.79	0.057	0.174
ORF23	−0.34	9.4	9.1	0.79	0.082	0.210
ORF25a	−0.37	8.2	7.9	0.77	*	0.115
ORF13a	−0.38	10.9	10.5	0.77	0.064	0.185
ORF1b	−0.39	6.7	6.3	0.76	0.174	0.328
ORF65	−0.39	6.4	6.0	0.76	0.124	0.267
ORF71	−0.41	7.0	6.6	0.75	0.090	0.210
ORF29	−0.42	7.5	7.1	0.75	*	0.125
ORF4a	−0.42	8.0	7.5	0.75	*	0.057
ORF34	−0.43	8.7	8.3	0.74	0.160	0.319
ORF41	−0.43	7.5	7.1	0.74	*	0.061
ORF48a	−0.46	10.7	10.2	0.73	**	0.053
ORF61	−0.48	11.5	11.0	0.72	*	0.115
ORF68	−0.49	10.9	10.4	0.71	**	*
ORF58	−0.50	11.1	10.6	0.71	**	*
ORF35	−0.52	7.4	6.9	0.70	0.142	0.299
ORF55	−0.53	8.6	8.1	0.69	0.088	0.210
ORF2a	−0.57	9.8	9.2	0.67	**	*
ORF21	−0.58	9.2	8.6	0.67	*	0.123
ORF50b	−0.62	11.1	10.5	0.65	**	**
ORF25b	−0.62	7.3	6.7	0.65	*	0.125
ORF56	−0.64	9.2	8.6	0.64	**	**
ORF3	−0.65	10.0	9.3	0.64	**	**
ORF59	−0.66	9.0	8.4	0.63	**	*
ORF52	−0.70	8.0	7.3	0.62	**	*
ORF33	−0.70	9.1	8.4	0.62	*	0.084
ORF60	−0.71	8.8	8.1	0.61	*	0.084
ORF2b	−0.73	9.4	8.7	0.60	**	**
ORF6	−0.75	6.9	6.2	0.60	0.109	0.241
ORF22	−0.86	9.2	8.4	0.55	**	*
ORF42	−0.97	10.5	9.5	0.51	**	**
ORF54	−1.00	8.8	7.8	0.50	**	**
ORF62b	−1.99	9.8	7.8	0.25	**	**
ORF14	−2.16	10.3	8.2	0.22	**	**

For each ORF, differential expression between Merck vaccine and parental Oka samples is shown in the first data column, calculated as $\bar{x}_{\text{Merck}} - \bar{x}_{\text{pOKA}}$, where the mean is taken over the log_2 scale normalised expression estimates obtained from five replicate samples for each sample type, which are shown in the next two columns. Data column four merely represents an antilogged version of the first data column, for readers who prefer this format. The penultimate data column contains the results from the statistical hypothesis testing, where each ORF was tested (empirical Bayes moderated *t*-test) for statistically different mean expression between the two sample types. The final column also shows statistical significance, but after controlling the false discovery rate that arises from testing multiple variables (ORFs) simultaneously. The table is sorted from highest up regulation to highest down regulation with respect to parental Oka

* $P \leq 0.05$

** $P \leq 0.01$

deviations of the complete set of 25 negative control spots. Differential expression ("log_2 fold change) for each probe is calculated, as the difference between mean log_2 expression for condition Y and mean log_2 expression for condition X. The statistical significance of mean expression between conditions is tested with empirical Bayes moderated *t*-tests. The statistical sample size for this purpose is $n = 5$ samples per condition. The sample size is not expected to provide self-conclusive evidence, but is considered sufficient to identify transcripts of interest for

Table 3 Differential transcription between parental Oka and GSK vaccine samples

	Log_2 fold change pOKA versus GSK vaccine	Log_2 expression pOKA	Log_2 expression GSK	Antilogged fold change	*P*-value	FDR *P*-value
ORF66	0.43	4.8	5.3	1.35	*	*
ORF36	0.36	4.3	4.6	1.28	0.090	0.101
ORF39	−0.07	7.2	7.1	0.95	0.704	0.712
ORF1b	−0.07	6.7	6.7	0.95	0.800	0.800
ORF30	−0.14	6.9	6.7	0.91	0.499	0.512
ORF1a	−0.20	6.9	6.7	0.87	0.369	0.383
ORF51	−0.21	5.8	5.6	0.86	0.224	0.236
ORF46b	−0.30	5.7	5.4	0.81	0.149	0.163
ORF43	−0.38	6.5	6.2	0.77	0.221	0.236
ORF19	−0.38	6.8	6.4	0.77	*	0.059
ORF31	−0.45	7.8	7.3	0.73	**	0.008
ORF26	−0.49	6.7	6.2	0.71	0.071	0.082
ORF12	−0.54	6.6	6.1	0.69	**	0.006
ORF67	−0.54	6.2	5.6	0.69	**	0.009
ORF5	−0.56	7.3	6.7	0.68	0.078	0.088
ORF11a	−0.56	6.3	5.7	0.68	*	*
ORF47	−0.57	6.8	6.2	0.67	**	**
ORF71	−0.61	7.0	6.4	0.65	*	*
ORF40	−0.65	8.0	7.4	0.64	**	**
ORF46a	−0.68	7.6	6.9	0.62	**	**
ORF4a	−0.71	8.0	7.3	0.61	**	**
ORF35	−0.71	7.4	6.7	0.61	*	0.059
ORF6	−0.72	6.9	6.2	0.61	0.120	0.133
ORF16	−0.75	8.3	7.6	0.60	**	**
ORF7	−0.81	12.0	11.2	0.57	**	**
ORF25b	−0.90	7.3	6.4	0.53	**	**
ORF18	−0.91	8.8	7.9	0.53	*	*
ORF25a	−0.92	8.2	7.3	0.53	**	**
ORF17	−0.98	8.7	7.7	0.51	**	**
ORF65	−1.00	6.4	5.4	0.50	**	**
ORF45	−1.00	8.2	7.2	0.50	**	**
ORF11c	−1.02	10.8	9.8	0.49	**	**
ORF10	−1.04	10.8	9.8	0.49	**	**
ORF49	−1.04	14.2	13.1	0.49	**	**
ORF52	−1.05	8.0	7.0	0.48	**	**
ORF56	−1.05	9.2	8.2	0.48	**	**
ORF2b	−1.05	9.4	8.4	0.48	**	**
ORF29	−1.11	7.5	6.4	0.46	**	**
ORF2a	−1.11	9.8	8.7	0.46	**	**
ORF41	−1.12	7.5	6.4	0.46	**	**
ORF37	−1.13	7.0	5.8	0.46	*	*
ORF70	−1.13	8.5	7.4	0.46	**	**
ORF4b	−1.16	9.4	8.2	0.45	**	**
ORF68	−1.20	10.9	9.7	0.44	**	**
ORF63	−1.25	12.2	10.9	0.42	**	**
ORF50b	−1.25	11.1	9.8	0.42	**	**
ORF20	−1.28	10.1	8.8	0.41	**	**

Table 3 continued

	Log_2 fold change pOKA versus GSK vaccine	Log_2 expression pOKA	Log_2 expression GSK	Antilogged fold change	*P*-value	FDR *P*-value
ORF15	−1.30	10.4	9.1	0.41	**	**
ORF9	−1.33	12.7	11.4	0.40	**	**
ORF50a	−1.38	11.6	10.2	0.39	**	**
ORF55	−1.39	8.6	7.2	0.38	**	**
ORF33	−1.41	9.1	7.7	0.38	**	**
ORF60	−1.47	8.8	7.3	0.36	**	**
ORF11b	−1.47	8.3	6.9	0.36	**	**
ORF48a	−1.49	10.7	9.2	0.36	**	**
ORF34	−1.50	8.7	7.2	0.35	**	**
ORF58	−1.52	11.1	9.5	0.35	**	**
ORF27	−1.55	11.5	10.0	0.34	**	**
ORF22	−1.58	9.2	7.7	0.34	**	**
ORF23	−1.58	9.4	7.8	0.33	**	**
ORF59	−1.60	9.0	7.4	0.33	**	**
ORF64	−1.62	12.4	10.8	0.33	**	**
ORF57	−1.63	12.4	10.8	0.32	**	**
ORF28	−1.67	9.3	7.6	0.31	**	**
ORF24	−1.67	12.5	10.8	0.31	**	**
ORF38	−1.68	11.6	9.9	0.31	**	**
ORF48b	−1.68	13.0	11.3	0.31	**	**
ORF61	−1.69	11.5	9.8	0.31	**	**
ORF13a	−1.71	10.9	9.2	0.31	**	**
ORF3	−1.74	10.0	8.2	0.30	**	**
ORF44	−1.74	8.3	6.6	0.30	**	**
ORF13b	−1.80	10.9	9.0	0.29	**	**
ORF32	−1.81	11.4	9.6	0.29	**	**
ORF69	−1.82	12.2	10.4	0.28	**	**
ORF54	−1.82	8.8	7.0	0.28	**	**
ORF8	−1.82	9.4	7.6	0.28	**	**
ORF21	−1.90	9.2	7.3	0.27	**	**
ORF42	−2.03	10.5	8.5	0.24	**	**
ORF62b	−2.18	9.8	7.6	0.22	**	**
ORF53	−2.23	11.5	9.3	0.21	**	**
ORF14	−2.42	10.3	7.9	0.19	**	**

For each ORF, differential expression between GSK vaccine and parental Oka samples is shown in the first data column, calculated as $\bar{x}_{GSK} - \bar{x}_{pOKA}$, where the mean is taken over the log_2 scale normalised expression estimates obtained from five replicate samples for each sample type, which are shown in the next two columns. Data column four merely represents an antilogged version of the first data column, for readers who prefer this format. The penultimate data column contains the results from the statistical hypothesis testing, where each ORF was tested (empirical Bayes moderated *t*-test) for statistically different mean expression between the two sample types. The final column also shows statistical significance, but after controlling the false discovery rate that arises from testing multiple variables (ORFs) simultaneously. The table is sorted from highest up regulation to highest down regulation with respect to parental Oka

* $P \leq 0.05$

** $P \leq 0.01$

further validation and comparison to existing literature. Since statistical tests are performed on multiple variables (probes) simultaneously, we also controlled the false discovery rate for the resulting *P*-values.

Results and discussion

The results of the array analysis for transcription of VZV ORFs on five sets of MeWo cells infected with either

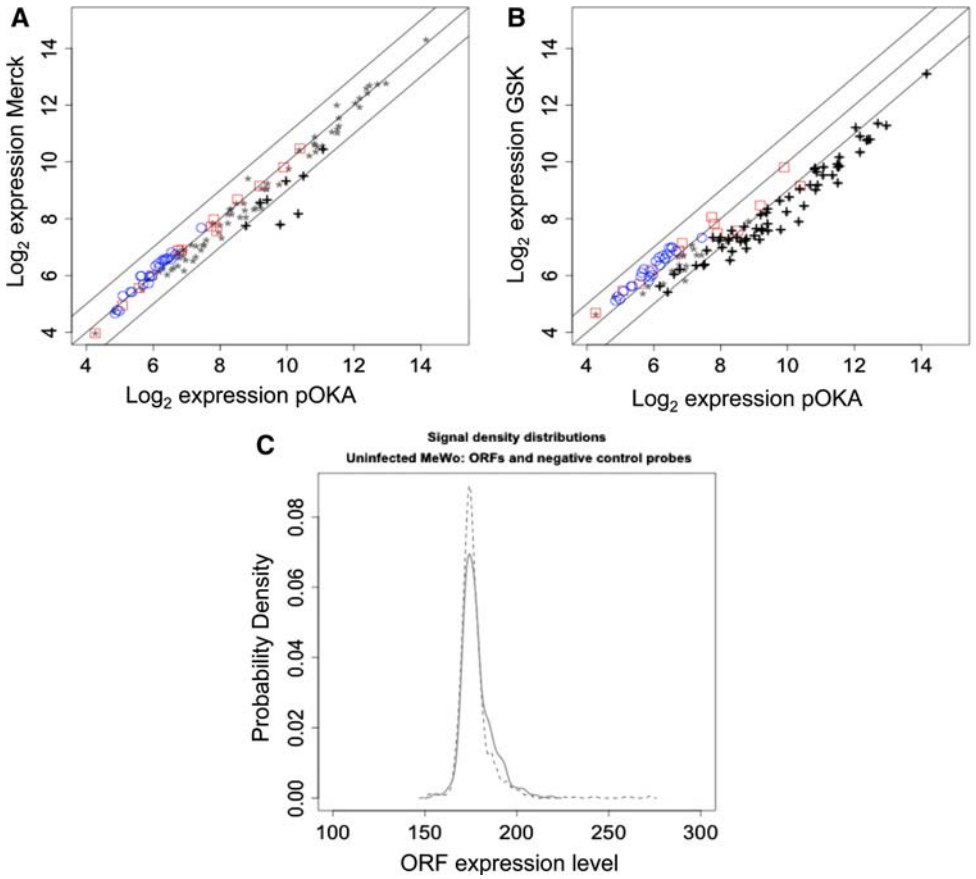

Fig. 1 Differential expression between parental Oka and vaccine samples. **a** Average expression level in parental OKA samples (*x*-axis) versus Merck vaccine samples (*y*-axis), based on five biological replicates each. Crosses represent significant (FDR controlled *P*-values ≤ 0.01) differentially expressed ORFs, grey asterisks all remaining ORFs, blue circles denote negative controls and red boxes positive controls. **b** Average expression level in parental OKA samples (*x*-axis) versus GSK vaccine samples (*y*-axis), based on five biological replicates each. Crosses represent significant (FDR controlled *P*-values ≤ 0.01) differentially expressed ORFs, gray asterisks all remaining ORFs, blue circles denote negative controls and red boxes positive controls. **c** Data distributions of ORFs (dotted line) and negative controls (solid line) in five uninfected samples (pilot study, data not shown). As expected, ORFs do not show a level of expression above negative controls

Merck or GSK vaccine viruses compared with P-Oka, and their statistical significance is shown in Tables 2 and 3, respectively, in decreasing order of their fluorescence intensity. There was a global downregulation of all transcription of both vaccines relative to the parental strain, although the extent of this downregulation was greater in the case of the GSK vaccine. This downregulation is evident in the scatter plot (Fig. 1) where the straight line represents equivalent transcription of VZV ORFs in a comparison of P-Oka to each of the vaccine strains. It can be seen that both ORF62 and ORF14 are the most transcriptionally downregulated overall for ORFs in both vaccines compared to the parental strain (summarised in Table 4 which also shows the values for ORF 31 which was not downregulated in the vaccines). The downregulation of ORF 14 was confirmed in GSK vaccine virus by dot blot analysis (data not shown), although it was not possible to confirm 62 downregulation by this method or by

Table 4 Relative expression shown as fold changes of 3 VZV ORFs in GSK and Merck Vaccine strains compared with parental P-Oka virus

ORF	GSK (fold change)	MERCK (fold change)
ORF14	−2.42	−2.16
ORF62	−2.18	−1.99
ORF31	−0.45	0.07

TaqMan, presumably related to differences in sensitivities of the techniques used. However, immunocytochemical analysis using antibodies to VZV ORF 14-encoded protein and ORF 62-encoded protein did confirm a reduced level of expression of both these proteins at 72 h post-infection in vaccine compared with P-Oka virus (Fig. 2, Box A). For both viruses, the values shown represent the expression of individual ORFs compared with all the other ORFs in the virus sample. However, this may possibly reflect the

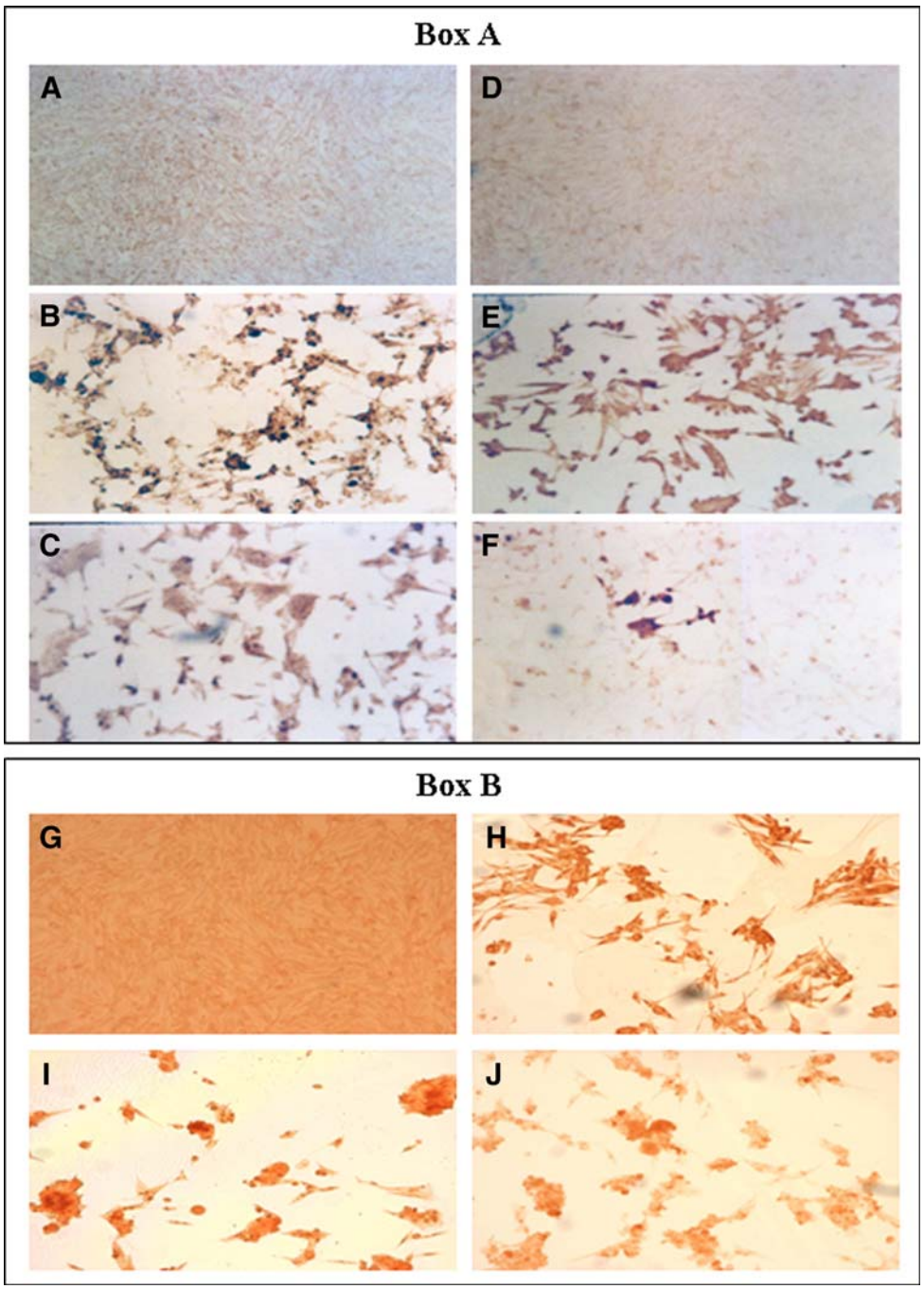

Fig. 2 **Box A** Immunostaining in MeWo cells for VZV ORF 14-encoded and ORF 62-encoded proteins following infection with P-Oka and GSK vaccine virus Uninfected control and VZV-infected MeWo cells at 72 h after infection with P-Oka or GSK vaccine virus were fixed and immunostained with a mouse monoclonal antibody to VZV ORF 62-encoded protein (Abcam) or a mouse monoclonal antibody to VZV ORF 14-encoded protein (a generous gift from Drs. J. Haas and S. Jonjic). Illustrations show anti-VZV ORF 14 staining on uninfected MeWo (panel A), MeWo infected with VZV P-Oka (panel B) and MeWo infected with GSK vaccine (panel C), and anti-VZV ORF 62 on uninfected MeWo (panel D), MeWo infected with VZV P-Oka (panel E) and MeWo infected with GSK vaccine (panel F). Results show a reduced level of 14 and 62 protein expression at 72 h in the GSK vaccine infected cells. The levels of infection in the different experiments were similar. Although there was some variation in staining intensity across the slides, representative views are shown. **Box B** Immunostaining in MeWo cells for VZV ORF 31-encoded protein following infection with P-Oka, Merck, and GSK vaccine strains. Uninfected control and VZV-infected MeWo cells at 72 h after infection with P-Oka, Merck or GSK vaccine virus were fixed and immunostained with a mouse monoclonal antibody to VZV ORF 13-encoded protein (a generous gift from Drs. J. Haas and S. Jonjic). Illustrations show anti-VZV ORF 31 staining on uninfected MeWo cells (panel G), MeWo infected with VZV P-Oka (panel H), MeWo infected with Merck vaccine (panel I), and MeWo infected with GSK vaccine (panel J). Results show similar intensities of ORF 31 protein staining for all three viruses. Levels of infection in the different experiments were similar, and representative views are shown

efficiency of the individual probe binding as well as any significant biological phenomenon. By contrast, the expression of ORF 31-encoded protein did not show any obvious differences on immunocytochemical analysis at 72 h in P-Oka compared with the two vaccine viruses (Fig. 2 Box B), consistent with the observation that ORF 31 on arrays was not downregulated in either of the vaccine viruses compared with P-Oka. In the case of the GSK vaccine, ORF53 was also significantly downregulated at similar levels to ORF62 and ORF14. We cannot be sure that this is biological fact or an artefact of the variation inherent in the data. The latter does not allow for perfect ranking in relation to the other ORFs.

The observed global quantitative shift downwards of gene expression in the two VZV vaccines compared with the P-Oka strain could represent either a greater virulence of P-Oka or else gene downregulation in the vaccines. To distinguish between these two possibilities we performed growth curve experiments on the three viruses at days 0, 1, 2, 3,-5, and 6 post-infection. Standard foci formation assays were performed and the results are shown in Fig. 3. The growth curve patterns were very similar for all three viruses indicating that one virus was not simply replicating more efficiently in culture than another. The similar in vitro growth patterns of the three viruses in the presence of global gene downregulation in both vaccine strains is an interesting finding, but this presumably indicates that the vaccines' clinical attenuation is reflected by the gene downregulation but that this does not necessarily correlate with altered viral growth characteristics in culture. The growth curves are perhaps slightly unusual in shape compared with a more usual linear curves but the precise reason(s) for this are not clear.

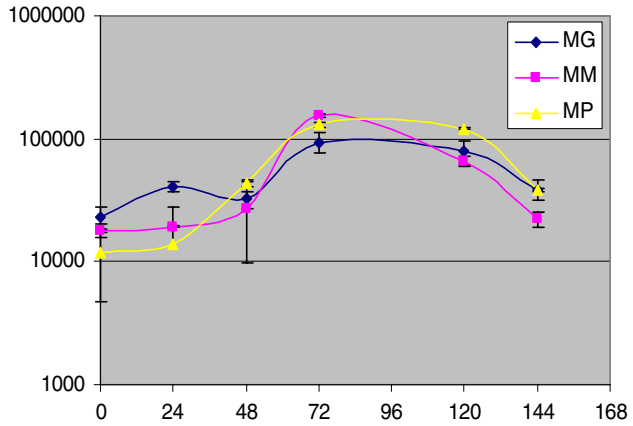

Fig. 3 Growth Curve Profiles of P-Oka (MP), Merck (MM), and GSK (MG) viruses [All three viruses were grown at 1–5 days after infection in MeWo cells. The *y*-axis shows the numbers of plaques counted (with standard deviations), and the *x*-axis shows the hours after infection. The growth curve patterns are very similar to each other]

This analysis has revealed differences in the transcriptomal profiles of the three viruses. In both GSK and the Merck vaccine viruses there was evidence of a global downregulation of transcription, consistent with the results of Cohrs et al. [12]. This downregulation was more extensive overall for GSK compared with Merck virus but the significance of this finding is as yet unclear. While we are aware of the intrinsic limitations of the small statistical sample size in the microarray analysis ($n = 5$ per group), the results of the growth curve experiments suggests that there were differences in the internal transcriptional regulation in the two vaccine strains compared with the parental P-Oka strain rather than any differences in the efficiency of viral replication in culture. We also used additional techniques to complement the microarray results. There was significant downregulation of transcription of ORFs 62 and 14 (encoding the major VZV transcriptional activator and glycoprotein C (gC), respectively) compared with the P-Oka strain. gC plays a crucial role in the virulence of VZV for human skin [13]. Diminished expression of gC has been proposed as a factor related to vaccine attenuation, but it has been shown that only a single synonymous change is present in ORF14 in the vaccine 6). Our finding of downregulation of gC is consistent with that found by Kinchington et al. [14] and Storlie et al. [15]. gC is not necessary for replication and has variable synthesis in tissue culture, but since all three viruses had equal passages in MeWo cells is it very unlikely that the differences seen in this study are due to tissue culture passage.

VZV ORF62 is essential for viral replication. Cohrs et al. [12] found no significant difference in the ability of vaccine derived ORF 62 protein to transactivate various promoters compared to the parental ORF 62. This contrasted with reports of Gomi and colleagues [16, 17] which indicated a reduced ability of V-Oka 62 protein to activate promoters of ORFs 28 and 29, but this may be attributable to the presence of regulatory sites external to the intergenic region. In addition, a recent study by Zerboni et al. [18], using chimeric Oka vaccine/parental Oka viruses suggests that ORFs 30–55 of pOka are sufficient to maintain wild-type infectivity in skin and, therefore, that mutations in various regions of the vaccine strains may be responsible for attenuation.

It is thought that there are 20 amino acid substitutions in vaccine compared to parental strain, affecting immediate-early, early and late proteins [8]. Previous studies have indicated that the vaccines contain mixtures of VZV genomes with varying genetic alterations which may have accumulated with increasing passages [8]. This may account for the differences in our results compared to those of Cohrs et al. [12] in which transcription of ORFs 65, 66, and 67 were also suppressed and transcription of ORF41 was elevated compared with P-Oka. In addition, genomic

differences have been reported between different lots of vaccine. Several strain variants with varied nucleotides coexist in vaccine lots, the vaccine continues to change in culture different seed lots may be used in preparations of the vaccines [19]. Long oligonucleotide VZV arrays provide a useful tool to analyse transcriptomal differences in viruses that have known phenotypic differences, but further experiments will be necessary to extend and elucidate these results, in particular the relative downregulation of ORFs 14 and 62. Differences at the level of translation and protein interactions will need to be further investigated to fully understand the mechanism of attenuation in VZV vaccines.

Acknowledgements This work was supported by a project grant to PGEK from the Chief Scientist Office (CSO) of Scotland. PGEK has acted on one occasion as a consultant to Sanofi Pasteur MSD.

References

1. R.J. Cohrs, D.H. Gilden, R. Mahalingam, Front. Biosci. **9**, 751–762 (2004). doi:10.2741/1275
2. P.G.E. Kennedy, E. Grinfeld, J.W. Gow, Proc. Natl. Acad. Sci. USA **95**, 4658–4662 (1998). doi:10.1073/pnas.95.8.4658
3. P.G.E. Kennedy, E. Grinfeld, J.E. Bell, J. Virol. **74**, 11893–11898 (2000). doi:10.1128/JVI.74.24.11893-11898.2000
4. P.G.E. Kennedy, Rev. Med. Virol **12**, 327–334 (2002). doi:10.1002/rmv.362
5. J.I. Cohen, S.E. Straus, A.M. Arvin, in *Fields Virology*, vol. 5, ed. by D.M. Knipe, P.M. Howley (Lippincott, Williams & Wilkins, Philadelphia, 2007), pp. 2773–2818
6. A.A. Gershon, P. LaRussa, I. Hardy, S. Steinberg, S. Silverstein, J. Infect. Dis. **166**(Suppl 1), S63–S68 (1992)
7. M.N. Oxman, M.J. Levin, G.R. Johnson, K.E. Schmader, S.E. Straus, L.D. Gelb, R.D. Arbeit, M.S. Simberkoff, A.A. Gershon et al., N. Engl. J. Med. **352**, 2271–2284 (2005). doi:10.1056/NEJMoa051016
8. Y. Gomi, H. Sunamachi, Y. Mori, K. Nagaike, M. Takahashi, K. Yamanishi, J. Virol. **76**, 11447–11459 (2002)
9. P.G.E. Kennedy, E. Grinfeld, M. Craigon, K. Vierlinger, D. Roy, T. Forster, P. Ghazal, J. Gen. Virol. **86**, 2673–2684 (2005)
10. A.J. Davison, J.E. Scott, J. Gen. Virol. **67**, 1759–1816 (1986). doi:10.1099/0022-1317-67-9-1759
11. T.D. Forster, D. Roy, P. Ghazal, J. Endocrinol. **178**, 195–204 (2003). doi:10.1677/joe.0.1780195
12. R.J. Cohrs, D.H. Gilden, Y. Gomi, K. Yamanishi, J.I. Cohen, J. Virol. **80**, 2076–2082 (2006). doi:10.1128/JVI.80.5.2076-2082.2006
13. J.F. Moffat, L. Zerboni, P.R. Kinchington, C. Grose, H. Kaneshima, A.M. Arvin, J. Virol. **72**, 965–974 (1998)
14. P.R. Kinchington, P. Ling, M. Pensiero, B. Moss, W.T. Ruyechan, J. Hay, J. Virol. **64**, 4540–4548 (1990)
15. J. Storlie, L. Maresova, W. Jackson, C. Grose, J. Infect. Dis. **197**(Suppl 2), S49–S53 (2008)
16. Y. Gomi, T. Imagawa, M. Takahashi, K. Yamanishi, J. Med.-Virol. **61**, 497–503 (2000). doi:10.1002/1096-9071(200008)61:4<497::AID-JMV13>3.0.CO;2-2
17. Y. Gomi, T. Imagawa, M. Takahashi, K. Yamanishi, Arch. Virol. Suppl. **17**, 49–56 (2001)
18. L. Zerboni, S. Hinchliffe, M.H. Sommer, H. Ito, J. Besser, S. Stamatis, J. Cheng, D. Distefano, N. Kraiouchkine, A. Shaw et al., Virology **332**, 337–346 (2005). doi:10.1016/j.virol.2004.10.047
19. A. Sauerbrei, R. Zell, M. Harder, J. Wutzler, J. Clin. Virol. **37**, 109–117 (2006). doi:10.1016/j.jcv.2006.07.002